Hilbert-Huang Transform versus Fourier based analysis for diffused ultrasonic waves structural health monitoring in polymer based composite materials

S.E. Hamdi[a], A. Le Duff[a], G. Plantier[a], L. Simon[b], R. El Guerjouma[b] and M.H. Ben Ghozlen[c]

[a]Groupe ESEO, rue Merlet de la Boulaye, 49009 Angers, France
[b]Laboratoire d'acoustique de l'université du Maine, Bât. IAM - UFR Sciences Avenue Olivier Messiaen 72085 Le Mans Cedex 9
[c]Faculté des Sciences de Sfax, Rte Soukra km 3.B.P. 1171, 3000 Sfax, Tunisia
seif-eddine.hamdi@eseo.fr

The use of time-frequency distributions for diffused signals analysis, which takes into account the non-stationarity of these signals, may be vital for structural health monitoring applications. Although this type of analysis may bring new information into the signals analysis, the interpretation of a time-frequency distribution may not be simple. In addition, the large number of available tools for time-frequency analysis with different assumptions about the signal features (i.e. assumptions about linearity, stationarity, etc.), may cause a problem when selecting the most appropriate technique for signal analysis, and then may affect the interpretation of results. In this paper, induced circular hole in a Glass Fiber Reinforced Polymer (GFRP) composite plate, considered as damages, are visualized on different time-frequency representations. In particular, representations obtained from traditional Fourier based analysis methods like spectrogram are compared to that provided by the Hilbert-Huang transform, recently developed. Such a comparison of these techniques can be very useful to justify the accuracy of the HHT and for guiding the choice of the appropriate monitoring strategy of a given process.

1 Introduction

Glass fiber reinforced polymer (GFRP) composite materials has been extensively used due to their attractive mechanical behavior, such as strength, stiffness, low weight, corrosion resistance, etc. These materials, as many other man-made structures, needs a better understanding of their damage mechanisms. Damages occurring in GFRP materials may be introduced in the manufacturing process or may be caused by environmental conditions or mechanical solicitations during the life-service of these structure. A key part of the analysis aims to identify the occurrence of a damage in GFRP materials for in situ health monitoring applications.

Diffused ultrasonic waves, formed after multiple reflections of an impulsive excitation from the structure boundaries, provides various advantages for damage monitoring. These waves propagate throughout the entire structure. In that way, a large material volume can be interrogated with a sparse array of transducers [1, 2].

Recently, the Hilbert-Huang Transform (HHT) [4, 6, 7], has been applied for non-stationary signals features analysis. Peng et al. [3] shows that the HHT can be an useful tool for both analysis and damage features extraction of vibration signal. In this paper, the HHT is used for detecting structural damage in polymer composite materials. an analysis of a GFRP composite plates containing a circular hole, in order to simulate damage, has been carried out. Finally, a damage detection performance comparison with a traditional Short Time Fourier Transform based analysis approach is performed.

The paper is structured as follows: In section 2, the principle of the HHT and the Short Time Fourier Transform are presented. In section 3, describes the experimental procedure. The diffused signals HHT based damage detection and the comparison results with the Fourier based analysis are discussed in section 4. In section 5, conclusions and future works are presented.

2 Details on the algorithms used

2.1 Principle of the HHT

The HHT, developed by Huang et al. [4, 5, 6, 7], is a time-frequency signal processing technique which was specially designed to analyze non-stationary data changes even within one oscillation cycle [8]. This method tends to empirically extract the intrinsic oscillation modes by their characteristic time scales in the data, and then to decompose data accordingly.

2.1.1 EMD method

The EMD decomposes signals into a set of intrinsic mode functions (IMFs) which represent simple oscillatory modes. Generally, the finest component of the shortest period at each instant will be identified and decomposed into the first IMF. The components of longer periods will be identified and decomposed into the following IMFs in sequence [9, 10]. The EMD method is based upon the assumption that any signal is composed from the contribution of different IMFs. For each one, it will assigned the same number of extrema and zero-crossings. There is only one extremum between successive zero-crossings. Each IMF should be independent of the others. In this way, each signal could be considered as the sum of a finite IMFs components, each of which must satisfy the following definition [5, 6, 7]:

1. In the whole data set, the number of extrema and the number of zero-crossings must either equal or differ at most by one;

2. At any point, the mean value of the envelope defined by local maxima and the envelope defined by the local minima is near zero.

The EMD decomposes data in a few steps. Hence, any signal $x(t)$ can be decomposed as follows [7]:

1. Identification of all the local extrema, then connecting all the local maxima by a cubic spline line as the upper envelope.

2. Repeating the same process for the local minima to produce the lower envelope. The upper and lower envelopes should cover all the data between them.

3. The mean value of upper and lower envelope is designated as m_1, and the difference between the signal $x(t)$ and m_1 is the first component, h_1, (figures 1 and 2). In that way, we have

$$x(t) - m_1 = h_1. \tag{1}$$

If h_1 satisfy the IMF requirements, then h_1 can be considered as the first component of $x(t)$.

4. If h_1 is not an IMF, it is treated as the original signal and repeat the steps 1-3; then

$$h_1 - m_{11} = h_{11}, \tag{2}$$

where, m_{11} is the mean of both upper and lower envelope value of h_1. This procedure is called sifting
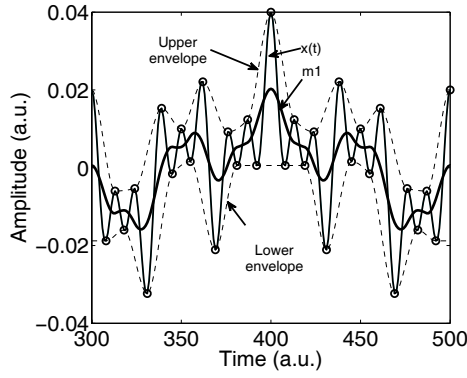
Figure 1: Sifting process: the original data $x(t)$ with the upper and the lower envelopes (dotted lines) and resultant mean line m_1 (bold line).
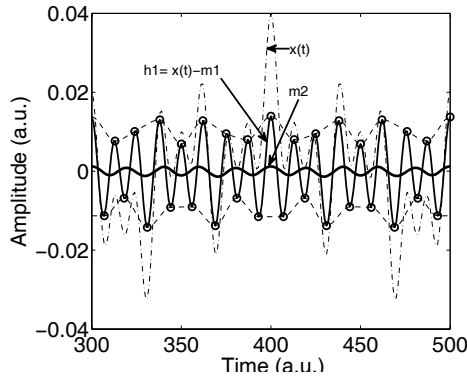

Figure 2: The data after the first sifting process.

process and is repeated, up to k times, on the successive data h_{ik} until the mean line between the upper and lower envelopes is near zero for any point. Then,

$$h_{1(k-1)} - m_{1k} = h_{1k}, \qquad (3)$$

and the first IMF component, designated as

$$c_1 = h_{1k}, \qquad (4)$$

represents the finest scale or the shortest period component of the signal $x(t)$.

5. Extracting c_1 from $x(t)$, leads to

$$r_1 = x(t) - c_1. \qquad (5)$$

The whole sifting process is repeated on r_1 for n times to obtain the successive components of increasing period. Then, n IMFs of signal $x(t)$ could be obtained. Hence,

$$r_{n-1} - c_n = r_n. \qquad (6)$$

When r_n becomes a monotonic function from which no more IMF can be extracted, then the decomposition process can be stopped. By cumulating (5) and (6)

$$x(t) = \sum_{j=1}^{n} c_j + r_n, \qquad (7)$$

where the last component r_n, treated as a residue, is the mean trend of $x(t)$. The IMFs $c_1, c_2, \ldots, c_n$ include different frequency bands ranging from high to

low. The frequency components contained in each frequency band are different and they change according to the variation of signal $x(t)$.

An IMF is a counter part to the simple harmonic function, but it is much more general: instead of constant amplitude and frequency, IMFs can have both variable amplitude and frequency as functions of time. This frequency-time distribution of the amplitude is designated as the Hilbert amplitude spectrum, or simply the Hilbert spectrum. Now, the next section deals with the Hilbert spectrum analysis.

2.1.2 Hilbert spectrum analysis

The Hilbert spectrum analysis provides a method for considering instantaneous frequency, which can be used for an accurate investigation of composite structures [11]. One of the easiest way to calculate the instantaneous frequency, $F_{i_{x(t)}}(t)$, is to apply the Hilbert transform. Indeed, for a real signal $x(t)$, it is possible to use the analytic signal $z(t)$ associated to $x(t)$,

$$z(t) = x(t) + jy(t) = a(t) \exp\left[j\theta(t)\right], \qquad (8)$$

in which,

$$a(t) = \sqrt{x^2(t) + y^2(t)}, \qquad (9)$$

$$\theta(t) = \arctan\left[\frac{y(t)}{x(t)}\right]. \qquad (10)$$

From equation 10, we can have the instantaneous frequency as

$$F_{i_{x(t)}}(t) = \frac{1}{2\pi} \frac{d\theta(t)}{dt}. \qquad (11)$$

After performing the Hilbert transform to each IMF component, the original time-series $x(t)$, can be expressed as the real part (RP) of $z(t)$:

$$x(t) = \sum_{i=1}^{n} a_i(t) \exp\left[j2\pi \int_0^T F_{i_{x(t)}}(t)t\right], \qquad (12)$$

in which T is entirely signal length. In equation 12, both amplitude, $a_i(t)$ and frequency $F_{i_{x(t)}}(t)$ of each component are presented as functions of time. This time-frequency distribution of the amplitude is designated as the Hilbert Spectrum (HS). Various forms of Hilbert spectra presentations can be made [7]. The Marginal Hilbert Spectrum (MHS), offers a measure of total energy contribution from each frequency value, i.e the MHS represents the cumulated amplitude over the entire data span [5, 7]. If more qualitative results are desired, the smoothed presentation of the Hilbert spectrum is preferred. In the smoothed form, the energy density and its trends of evolution as functions of frequency and time are easier to identify. Several smoothing methods can be applied [5]. In this work, a 15×15 weighted Gaussian filter will give the Smoothed Hilbert Spectrum (SHS).

2.2 Short-Time Fourier Transform

One of the most used time-frequency representations of a time signal is known as Short Time Fourier Transform (STFT). The STFT basic idea is a moving window Fourier Transform [13, 14]. The time domain moving window over the signal generates a 2-D time-frequency distribution called spectrogram. The STFT of a signal $x(t)$ is defined as
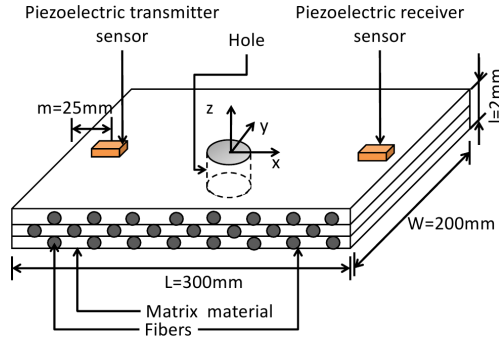
Figure 3: GFRP composite plate with a circular hole.

$$STFT(t,F) = \int_{-\infty}^{+\infty} x(\tau)w(\tau-t)\exp(-j2\pi F\tau)d\tau, \quad (13)$$

in which $w(\tau-t)$ is the moving window. Many window functions are used, each of them at different application [13]. Some of them are known as Hamming, Hanning, Kaiser-Bessel and Gaussian windows. In this paper, Hamming window is used for the analysis of the diffused ultrasonic waves.

3 Experimental procedure

The experimental work is carried out on a GFRP plate in order to acquire diffuse ultrasonic signals under damaged and undamaged conditions. GFRP composite samples noted 0_8° are fabricated. The stacking sequence consists of 8 layers of unidirectional reinforcement. A circular hole of 5 mm diameter was introduced in the middle of the GFRP sample in order to simulate damage. Two piezoelectric sensors were mounted on the GFRP sample as shown in figure 3, and secured with small clamps. The sensors used, for the generation and the reception of diffused waves, are a broadband sensors with an operating frequency range lying from 100 kHz to 1 MHz. The excitation signal $e(t)$ is a sinusoidal burst composed of a single period frequency around 100 kHz. This excitation is repeated each 20 ms, and provided by an Agilent 33220A function generator. The reception is provided through a Nicolet Sigma 100 acquisition system. This system allows the registration of 100,000 samples of the received signal at a sampling frequency of 10 MHz. In order to improve the signal to noise ratio, the received signal, is collected after an averaging of 100 acquisitions. The geometry of the GFRP samples, the hole and the sensors locations are given in figure 3.

4 Results and discussion

4.1 Time-frequency investigation of a synthetic time-varying signal

A synthetic signal, $f(t)$, was created to simulate time-varying dominant frequencies which may be faced in diffused signal measurements. The test signal is composed of four changing sinusoidal waves with different frequencies interfering (figure 4).
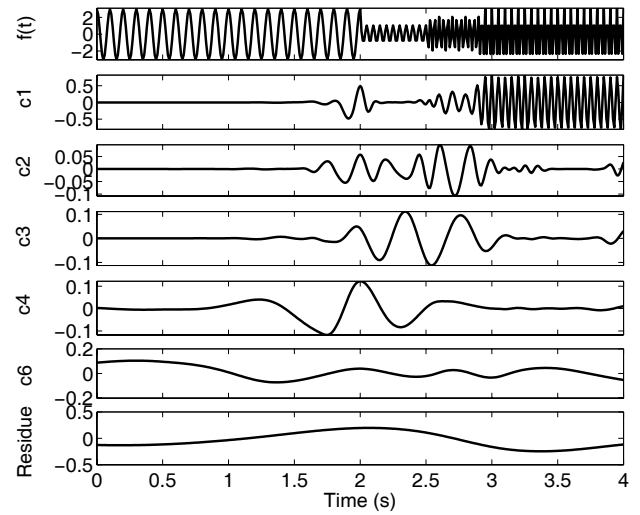
Figure 4: Test signal $f(t)$ and its IMFs components.
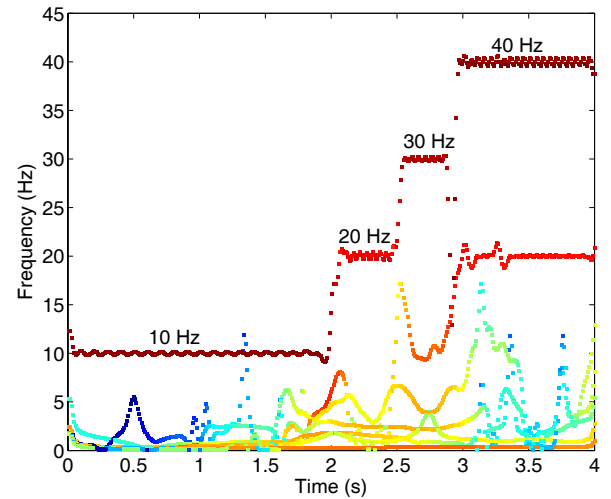
Figure 5: Hilbert spectrum of $f(t)$.

$$f(t) = \begin{cases} 3 \times \cos(2\pi 10t); & 0\ \text{s} \le t < 2\ \text{s} \\ 1 \times \cos(2\pi 20t); & 2\ \text{s} \le t < 2.5\ \text{s} \\ 2 \times \cos(2\pi 30t); & 2.5\ \text{s} \le t < 2.9\ \text{s} \\ 3 \times \cos(2\pi 40t); & 2.9\ \text{s} \le t < 4\ \text{s} \end{cases}$$

The HS of $f(t)$ is shown in figure 5. As may be seen, the HHT gives very sharp time-frequency representation of the oscillating components of the synthetic signal $f(t)$. The frequency gap occurred around 2s and 4s is well detected. The HS representation shows the presence of oscillatory modes located at low frequencies. This is due to that the HHT is a data driven process. The most energetic signal components are located at the first IMFs. The results using this method were compared to these obtained by the STFT method. The time-frequency representation is provided in figure 6. The time-frequency resolution of STFT depends on the window function length. A narrower window, (figure 6a), gives good time resolution but poor frequency resolution. A wide window, (figure 6c), gives better frequency resolution but poor time resolution.
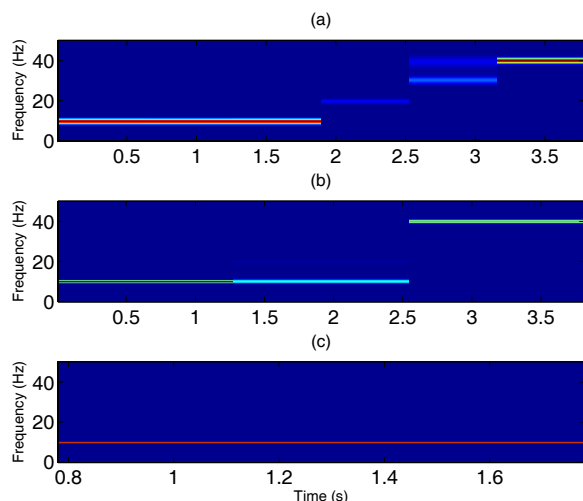
Figure 6: Results of test signal analysis using STFT with different window function length: ((a)- 0,64 s, (b)- 1.28 s, (c)- 2.56 s).
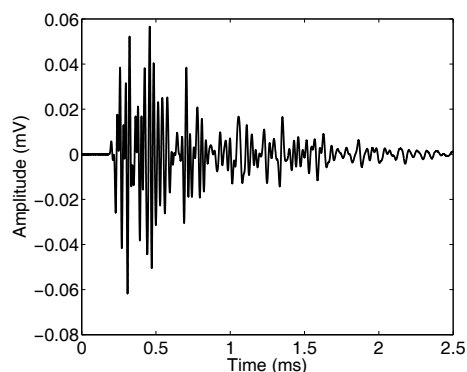

Figure 7: The received diffused signal from the undamaged GFRP sample.

4.2 Hole detection in GFRP composite plate

In this part of the paper, the performance of both HHT and the STFT methods for detecting a hole damage in a GFRP plate is discussed. Figures 7 and 8, show the diffused signal waveforms from the undamaged and the damaged GFRP sample, (before and after introducing a circular hole), respectively. In the case of the damaged case, the acquired signals takes more time to reach the receiver then those acquired from the undamaged case due to the introduced hole (figure 8).

The visualization of the results of the HHT based analysis of the both previous signals are presented, in figures 9 and 10 respectively. The time-frequency representation by means of the SHS of the diffused signal from the undamaged sample (figure 9) shows the presence very low frequency components located at the beginning of the signal waveform. Meanwhile, in the case of the damaged sample, the SHS representation shows the presence of a significant frequency component due to the introduced hole. This frequency signature, located around 180 kHz, is stretched along the signal waveform (figure 10).

The STFT method is applied for the analysis of the same previous signals. The visualization of the results of the time frequency distribution of these signals, is presented in fig-
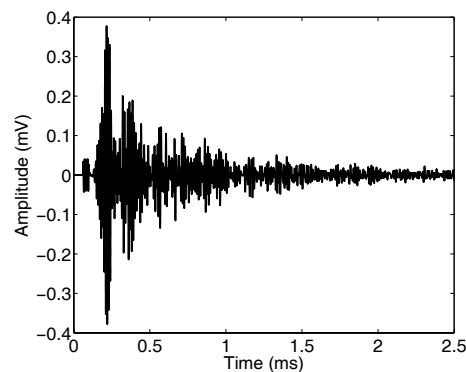

Figure 8: The received diffused signal from the damaged GFRP sample.
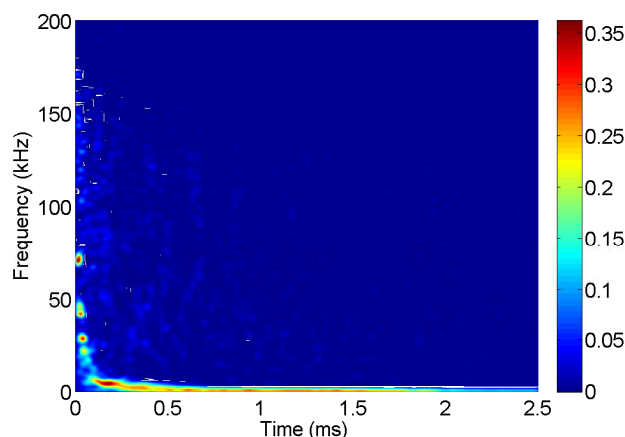

Figure 9: SHS of diffused signal from the undamaged GFRP sample.

ures 11 and 12. As may be seen, in the case of the undamaged sample, the STFT presents a frequency signature located around 400 kHz (figure 11). The hole occurrence is also detected by the presence of a second frequency component around 180 kHz (figure 12). Hence, it can be concluded that the hole presence generate a frequency signature which is estimated at around 180 kHz. Meanwhile, contrary to the HHT analysis, which does not need any pre-processing steps, the spectrogram provided by STFT is time-frequency limited in resolution. During the STFT processing, the results are not good in both time and frequency domain. In addition, any signal component, whose time duration is smaller than the time duration of the window decomposition, is disappeared after the transform of the signal.

5 Conclusion

A time-frequency analysis of non-stationary diffused signals has been conducted. The accuracy of the HHT as a tool for both analysis and damage detection in GFRP composite materials has been provided by a simultaneous STFT based analysis. This procedure shows a better time-frequency resolution for HHT method then the STFT based analysis. Meanwhile, it is not eligible to say such signal processing technique has a right or wrong time-frequency decomposition. The must important is whether the method being applied is useful or not useful for the specific application. The HHT is
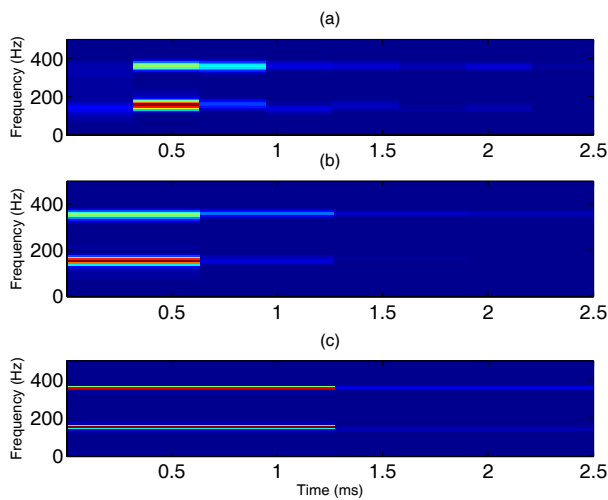
Figure 12: Diffused signal analysis from the damaged GFRP sample using STFT with different window function length: ((a)- 0,64 s, (b)- 1.28 s, (c)- 2.56 s).
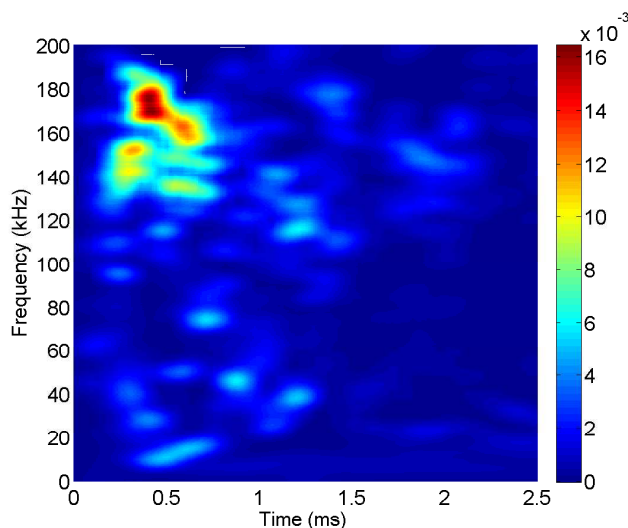

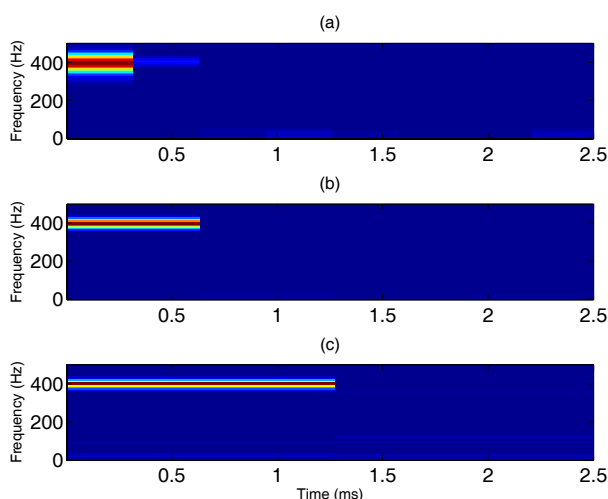Figure 10: SHS of diffused signal from the damaged GFRP sample.

Figure 11: Diffused signal analysis from the undamaged GFRP sample using STFT with different window function length: ((a)- 0,64 s, (b)- 1.28 s, (c)- 2.56 s).

a data driven signal processing technique with far less pre-processing steps then traditional methods. In that way, the HHT may be attractive for in situ structural health monitoring applications.

References

[1] Y. Lu, J. E. Michaels, "A methodology for structural health monitoring with diffuse ultrasonic waves in the presence of temperature variations" *Ultrasonics*, **43** 717-731, (2005)

[2] J. E. Michaels, T. E. Michaels, "Detection of structural damage from the temporal coherence of diffuse ultrasonic signals" *IEEE Transactions on Ultrasonics, Ferroelectrics and Frequency Control*, (2005)

[3] Z. Peng, P. Tse, F. Chua, "An improved Hilbert-Huang transform and its application in vibration signal analysis" *Journal of Sound and Vibration Volume* **286** 187-205, (2005)

[4] N. E. Huang, S. R. Long, Z. Shen. "The mechanism for frequency down-shift in nonlinear wave evolution", *Advances in Applied Mechanics* **32**, 59-117, (1996)

[5] N. E. Huang, Z. Shen, S. R. Long, M. C. Wu, H. H. Shih, Q. Zheng, N. C. Yen, C. C. Tung, H. H. Liu, "The empirical mode decomposition and the Hilbert spectrum for nonlinear and non-stationary time series analysis", *Proceedings of the Royal Society A Mathematical Physical and Engineering Sciences* 903-995, (1998)

[6] N. E. Huang, Z. Shen, S. R. Long, "A new view of nonlinear water waves: The Hilbert spectrum", *Annual Review of Fluid Mechanics* **31**, 417-457, (1999)

[7] N. E. Huang, "Introduction to the Hilbert-Huang Transform and its related mathematical problems", *Hilbert-Huang Transform and its applications* 324-331, (2005)

[8] R. Kazys, O. Tumsys, D. Pagodinas, "Ultrasonic detection of defects in strongly attenuating structures using the Hilbert-Huang transform", *NDT &E International* **41**, 457-466, (2008)

[9] C. C. Lin, P. L. Liu, P. L. Yeh, "Application of empirical mode decomposition in the impact-echo test", *NDT &E International* **42**, 589-598, (2009)

[10] S. Loutridis, E. Douka, L. J. Hadjileontiadis, "Forced vibration behaviour and crack detection of cracked beams using instantaneous frequency", *NDT &E International* **38**, 411-419, (2005)

[11] L. Lin, F. Chu, "Feature extraction of AE characteristics in offshore structure model using Hilbert-Huang transform", *Measurement* **44**, 46-54, (2011)

[12] National Instruments Corporation. NI PXI-1045 User Manual. p63, (2005)

[13] L. Cohen, "Time-frequency analysis: Theory and Applications" *New York: Prentice-Hall*, p320, (1995)

[14] P. Flandrin, "Time-frequency/time-scale analysis" *Academic Press Inc*, p386, (1999)